

SUPPLEMENTARY INFORMATION

Histamine deficiency promotes inflammation-associated carcinogenesis through reduced myeloid maturation and accumulation of CD11b⁺Ly6G⁺ immature myeloid cells

Xiang Dong Yang¹, Walden Ai^{1,7}, Samuel Asfaha¹, Govind Bhagat², Richard A. Friedman³, Guangchun Jin¹, Heuijoon Park¹, Benjamin Shykind⁴, Thomas G Diacovo⁵, Andras Falus⁶, Timothy C Wang¹

¹Division of Digestive and Liver Diseases, Department of Medicine and Irving Cancer Center, Columbia University, New York, NY 10032;

²Department of Pathology and Cell Biology, Columbia University;

³Department of Biomedical Informatics, Columbia University;

⁴Department of Neuroscience, Columbia University;

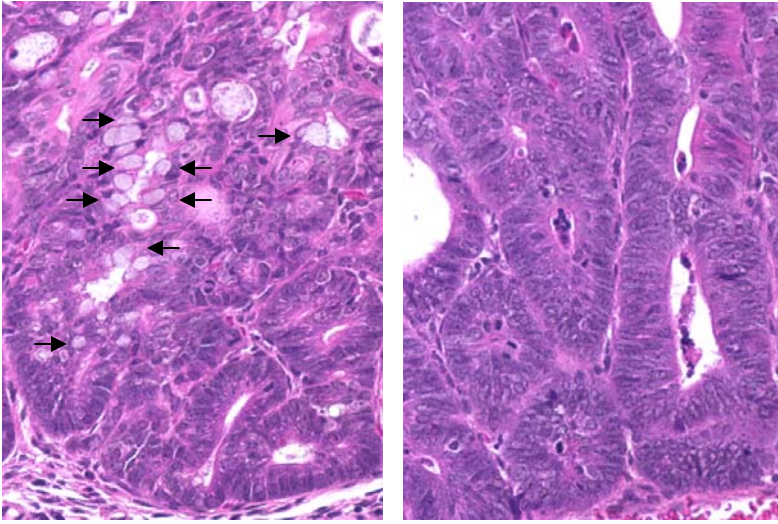
⁵Department of Pediatrics, Columbia University;

⁶Department of Genetics, Cell and Immunobiology, Semmelweis University, H-1089 Budapest, Hungary;

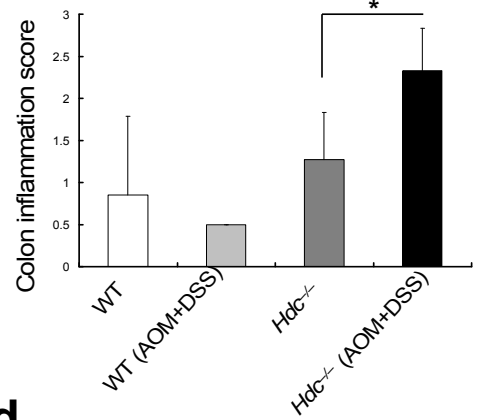
⁷Department of Pathology, Microbiology and Immunology, University of South Carolina School of Medicine, Columbia, SC 29208.

Supplementary Figures 1-17

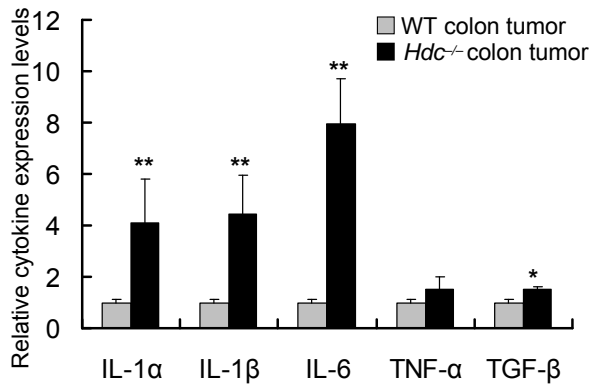
a WT (colon adenoma) *Hdc*^{-/-} (colon carcinoma)



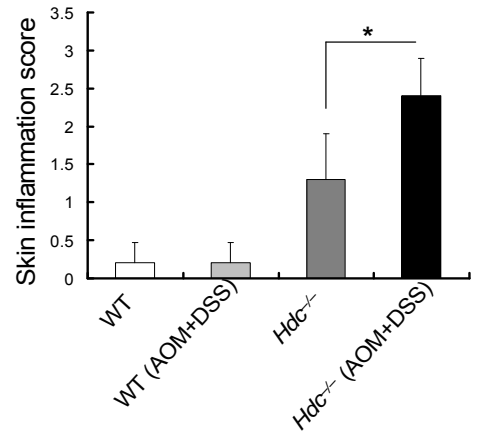
b



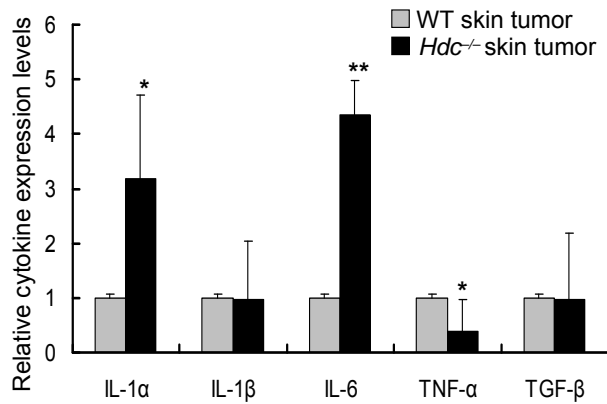
c



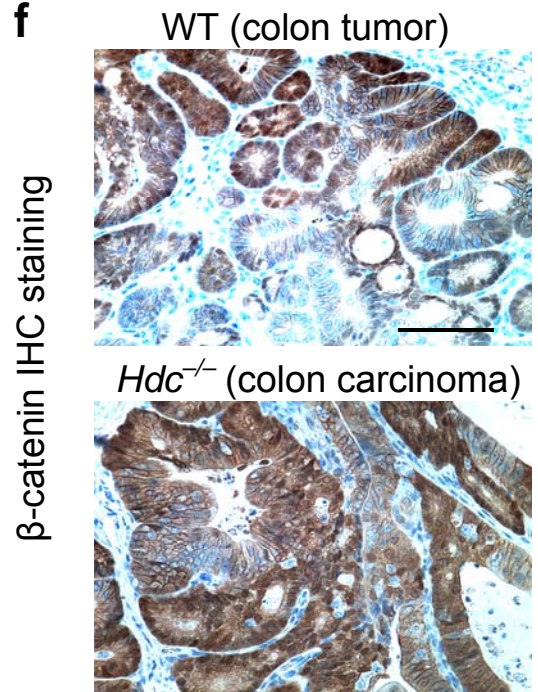
d



e

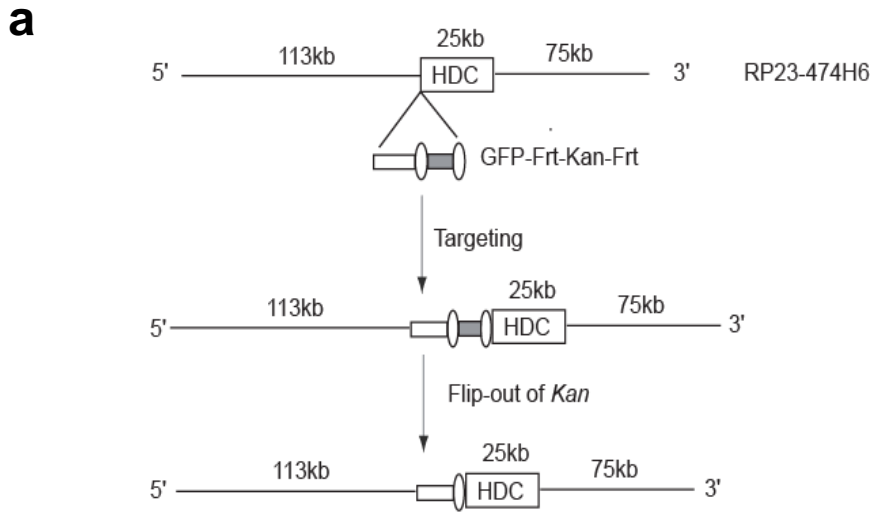


f

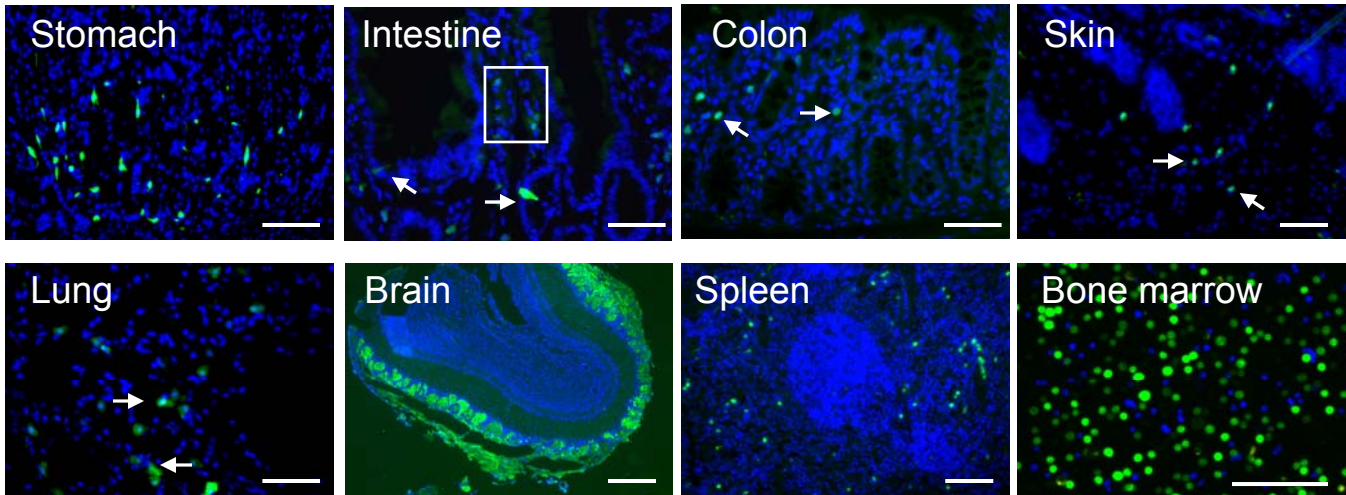


Supplementary Figure 1. *Hdc*^{-/-} mice show greater inflammatory response to carcinogens.

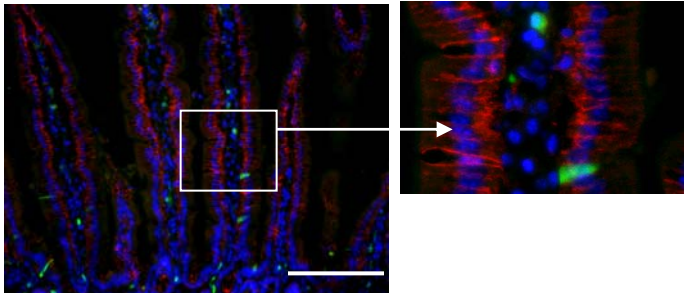
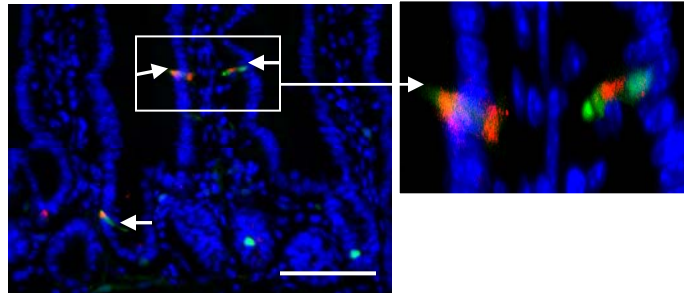
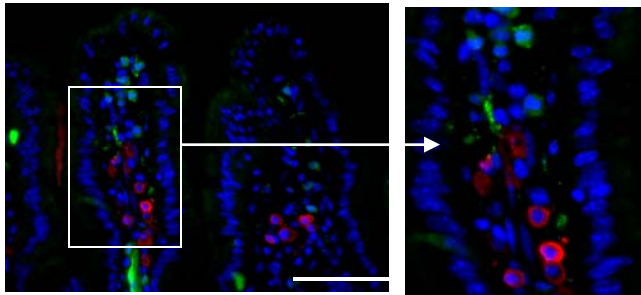
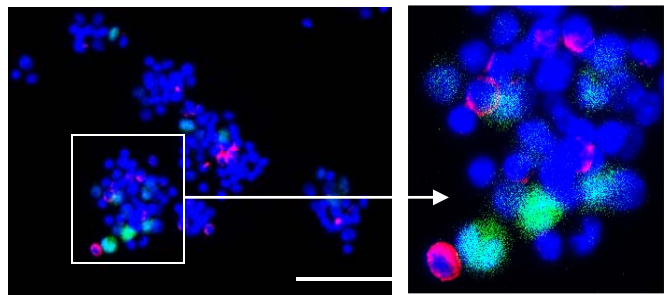
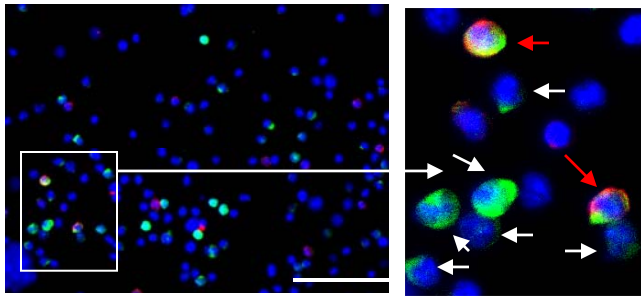
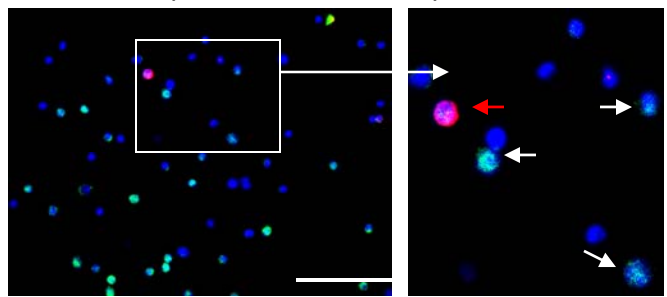
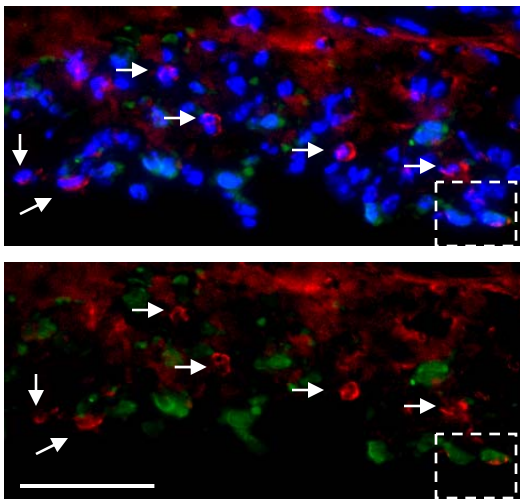
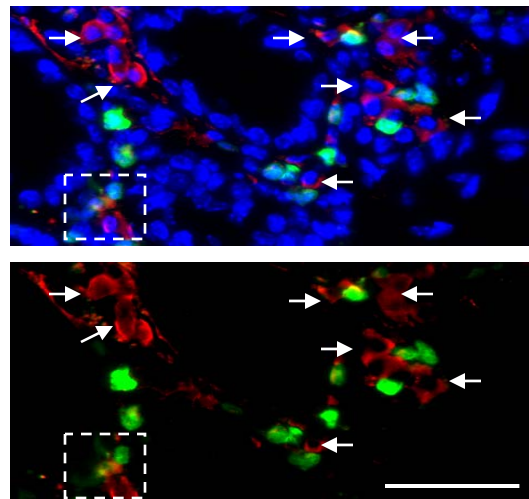
(a) Hematoxylin and eosin staining of colonic adenomas from wildtype mice and adenocarcinomas from *Hdc*^{-/-} mice treated with AOM + DSS. Blank arrows indicate goblet cells in the colonic tumors of wildtype mice. (b) and (d) Inflammation scores of colon and skin tumors following a carcinogenic stimulus. (b) Colonic tissues from *Hdc*^{-/-} mice after AOM + DSS treatment exhibit a greater inflammation score (* $P < 0.05$; mean \pm s.d. $n = 8$, each group). (d) Inflammation scores were elevated in the skin of *Hdc*^{-/-} mice treated with DMBA + TPA treatment. Inflammation scores were calculated using a semiquantitative scoring system⁵⁰ (* $P < 0.05$, mean \pm s.d. $n = 5$, each group). (c) and (e) Inflammatory cytokine expression in colonic (c) and skin (e) tumors of *Hdc*^{-/-} mice was measured by Q-RT-PCR and compared to wildtype mice in both the AOM + DSS or DMBA + TPA models (* $P < 0.05$; mean \pm s.d. $n = 5$, each group). (f) Immunohistochemistry staining for beta-catenin in colonic tumors from wildtype and *Hdc*^{-/-} mice (The images are representative of data from five colon tumors).



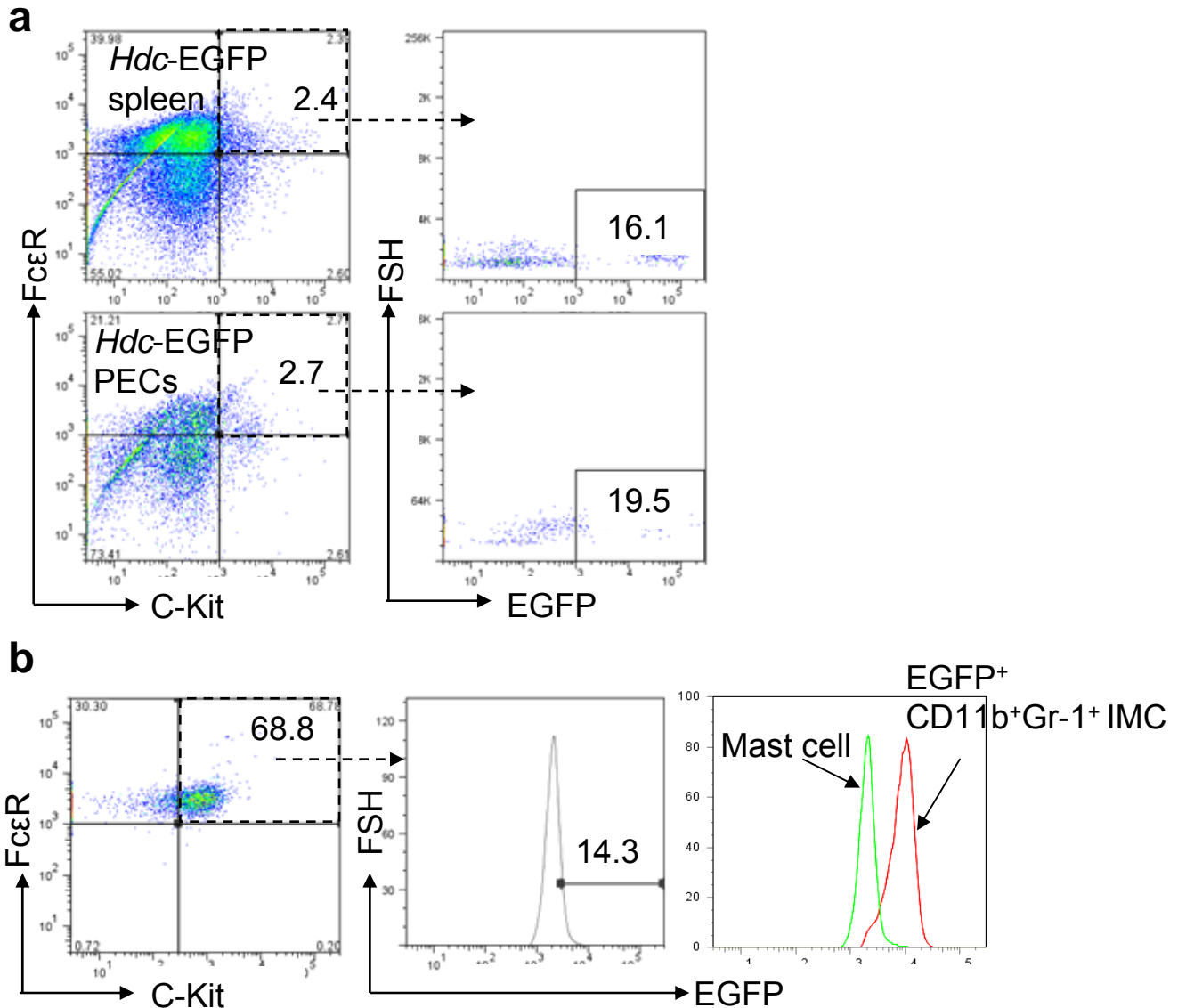
b



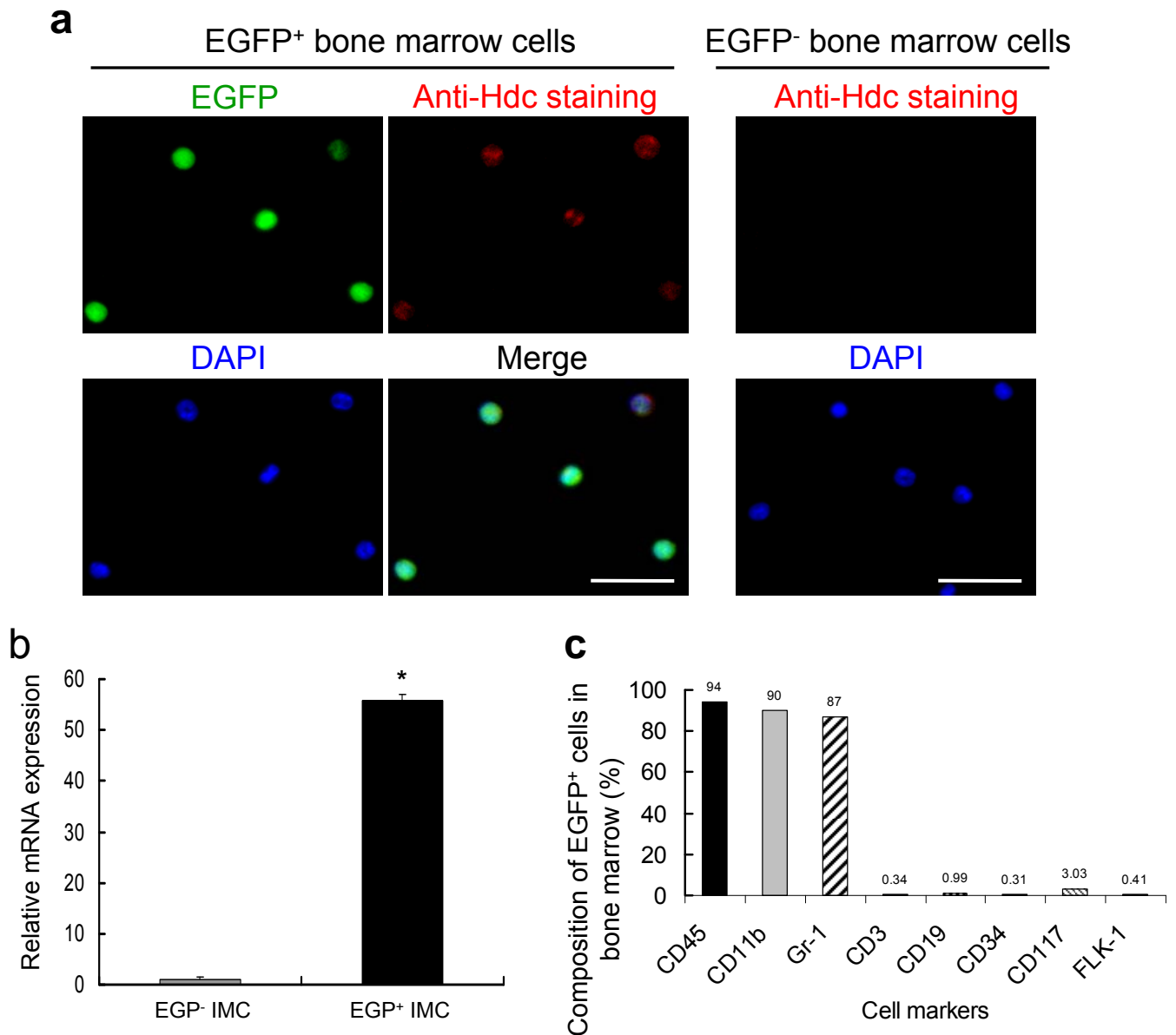
Supplementary Figure 2. Generation of *Hdc*-EGFP BAC transgenic mice. (a) Schematic depiction of the *Hdc*-EGFP BAC construct. A PCR generated fragment comprising the EGFP cDNA (smaller rectangle) and the Kanamycin resistance gene cassette (gray box) flanked by two Frt sequences was inserted into the mouse *Hdc* gene (shown by the large rectangle)-containing BAC clone (RP23-474H6) at the *Hdc* translation start site by homologous recombination. This BAC clone contains ~113 kb 5' and ~75 kb 3' flanking DNA. The Kanamycin resistance cassette was subsequently removed by FLP recombinase. (b) Fluorescence microscopy showing tissue-specific EGFP expression in *Hdc*-EGFP mice. Representative EGFP fluorescence with DAPI counterstaining in the stomach, small intestine, colon, skin, lung, brain, spleen, and bone marrow of adult 3-month old *Hdc*-EGFP mice are shown.

a E-cad/EGFP/DAPI**b** CgA/EGFP/DAPI**c** Tryptase/EGFP/DAPI (Intestine)**d** Tryptase/EGFP/DAPI (PEC)**e** Tryptase/EGFP/DAPI
(BM of *Hdc*-EGFP)**f** Tryptase/Hdc/DAPI
(BM of WT mice)**g** c-Kit/EGFP/DAPI (skin with TPA)**h** c-Kit/EGFP/DAPI (Colon tumor)

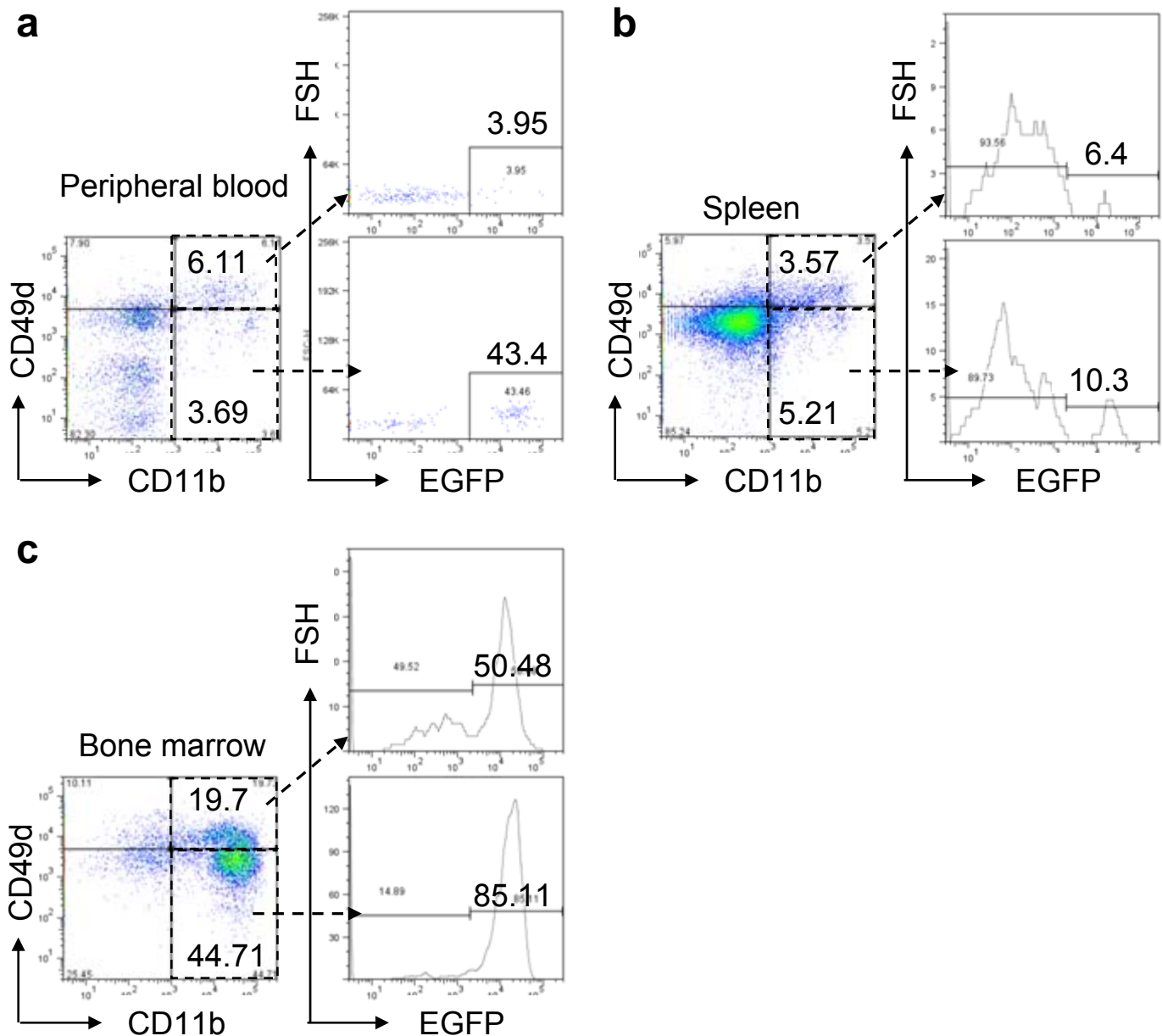
Supplementary Figure 3. *Hdc*-EGFP expression is absent in the anti-tryptase positive mast cells of peripheral organs. (a) EGFP⁺ cells are observed in both the intestinal epithelium and submucosa. E-cadherin (E-cad)-specific antibody staining shows co-localization in EGFP⁺ epithelial cells (indicated by the narrow arrows →) but no co-localization in EGFP⁺ submucosal cells. (b) Chromogranin A (CgA)-specific antibody staining demonstrates that EGFP⁺ epithelial cells in the intestine are endocrine cells. (c) Tryptase-specific antibody staining reveals a lack of co-localization in submucosal EGFP⁺ cells in the intestine. (d) Tryptase-specific antibody staining shows rare co-localization with EGFP expression in peritoneal exudative cells (PECs). (e) and (f) Bone marrow cells were flushed from the femur of *Hdc*-EGFP (e) and wildtype (f) mice and fixed with 2% *Paraformaldehyde* solution. In (e), Tryptase-specific antibody staining (Texas Red) of bone marrow cells from *Hdc*-EGFP mice shows some co-localization with EGFP expression in occasional immature mast cells. (f) Tryptase (Texas Red) and Hdc (FITC)-specific antibody double stained bone marrow-derived cells of wildtype mice confirmed that rare immature mast cells express Hdc. A large number of EGFP⁺ cells are indicated by the white arrow and less EGFP⁺ and anti-tryptase⁺ mast cells indicated by the red arrow. (g) and (h) c-Kit (CD117)-specific antibody staining reveals rare co-localization (approximately 10%) with EGFP⁺ cells in the dermis treated with TPA (g) and in the stromal of colon tumor induced by AOM + DSS (h). (Arrows indicate c-Kit positive cells and in box shows EGFP⁺c-Kit⁺ double positive cells. (The images are representative of data from three independent experiments).



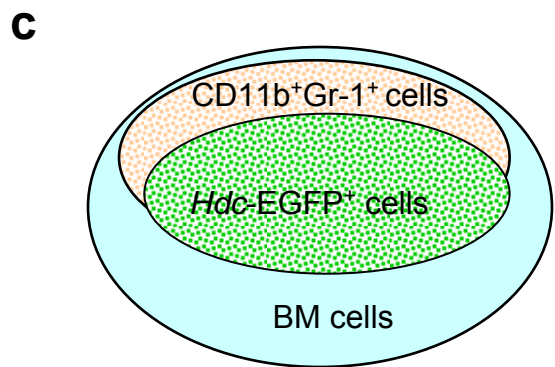
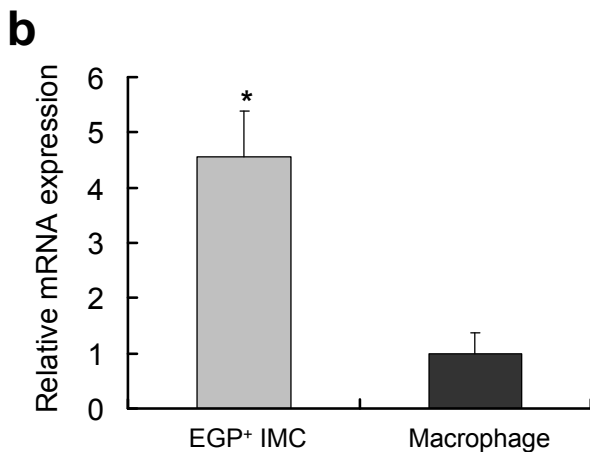
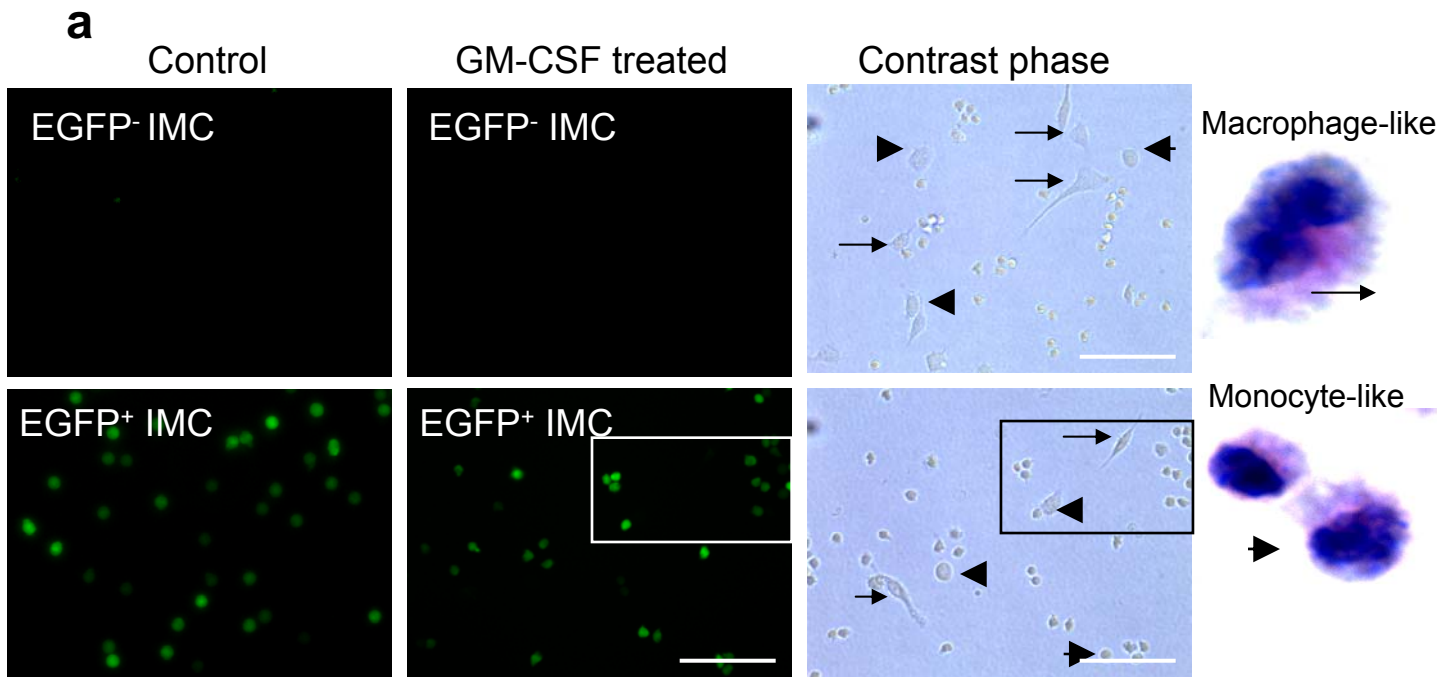
Supplementary Figure 4. *Hdc*-EGFP expression is repressed in the $c\text{-Kit}^+\text{Fc}\epsilon\text{R}^+$ mast cells of peripheral organs. (a) $c\text{-Kit}^+\text{Fc}\epsilon\text{R}^+$ mast cells are gated from the spleen (top) and peritoneal exudates cells (PEC, bottom) of *Hdc*-EGFP mice (left panel) and further analysis indicates the proportion of EGFP⁺ cells in the $c\text{-Kit}^+\text{Fc}\epsilon\text{R}^+$ mast cells (Representative FACS data is from five *Hdc*-EGFP mice). (b) *Hdc*-EGFP expression was repressed in IL-3 dependent $c\text{-Kit}^+\text{Fc}\epsilon\text{R}^+$ mast cells. Bone marrow cells were flushed from the femur of *Hdc*-EGFP mice and cultured in conditional medium with IL-3 (10 ng ml⁻¹) for four weeks. EGFP-expressing CD11b⁺Gr-1⁺ IMCs were sorted and cultured as a control. The FACS data is representative of data from three independent experiments.



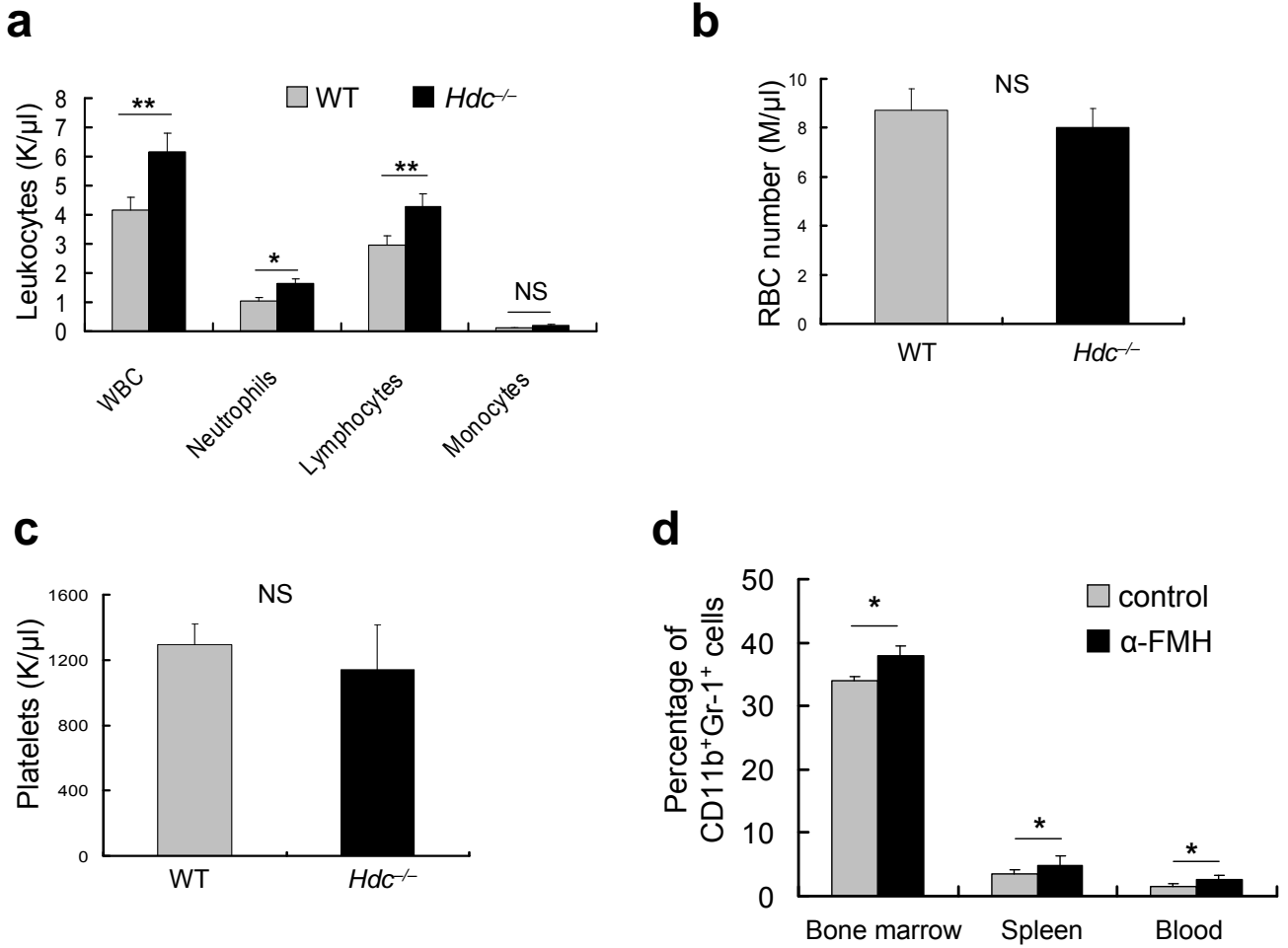
Supplementary Figure 5. *Hdc*-EGFP expression is deficient in EGFP⁻ myeloid cells within the bone marrow. (a) Co-localization of EGFP and *Hdc* expression in bone marrow cells. EGFP⁺ and EGFP⁻ cells were sorted from the bone marrow of *Hdc*-EGFP mice and fixed with 2% *paraformaldehyde* solution. *Hdc*-specific antibody stained cells with DAPI counterstain are shown. The images are representative of data from three independent experiments. (b) *Hdc* mRNA expression in EGFP⁻ and EGFP⁺ bone marrow myeloid cells. Quantitative RT-PCR analysis shows high levels of *Hdc* mRNA in EGFP⁺ bone marrow-derived cells (* $P < 0.001$; mean \pm s.d. $n = 3$). (c) Characterization of cell surface markers on EGFP⁺ bone marrow cells. FACS analysis of EGFP⁺ cells for hematopoietic lineage markers CD45, CD3, CD19, CD11b, Gr-1, CD34, c-kit (CD117) and FLK-1. Most EGFP-expressing cells were CD45⁺, CD11b⁺ and Gr-1⁺ but negative for other markers. The data represent measurements from five mice.



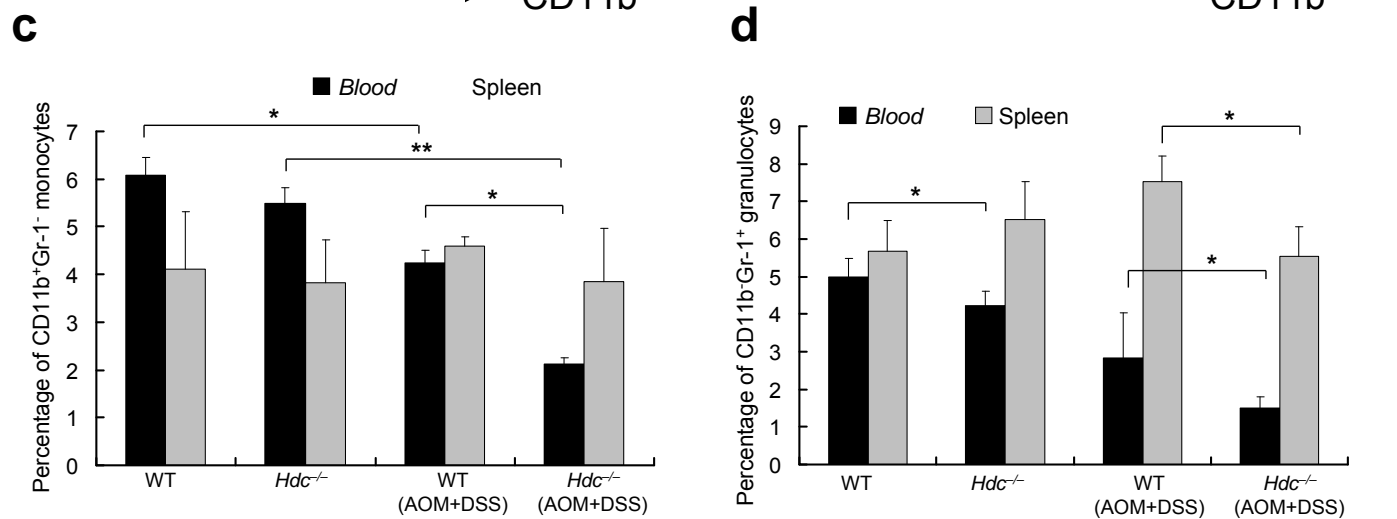
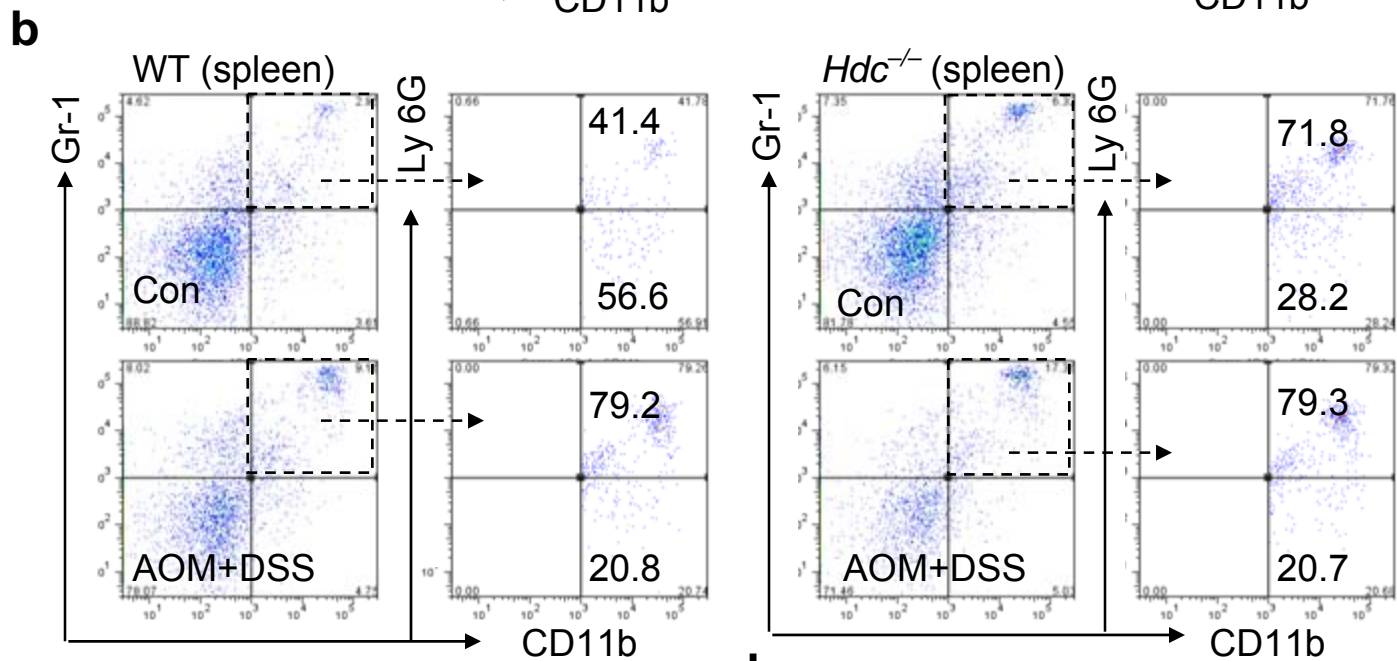
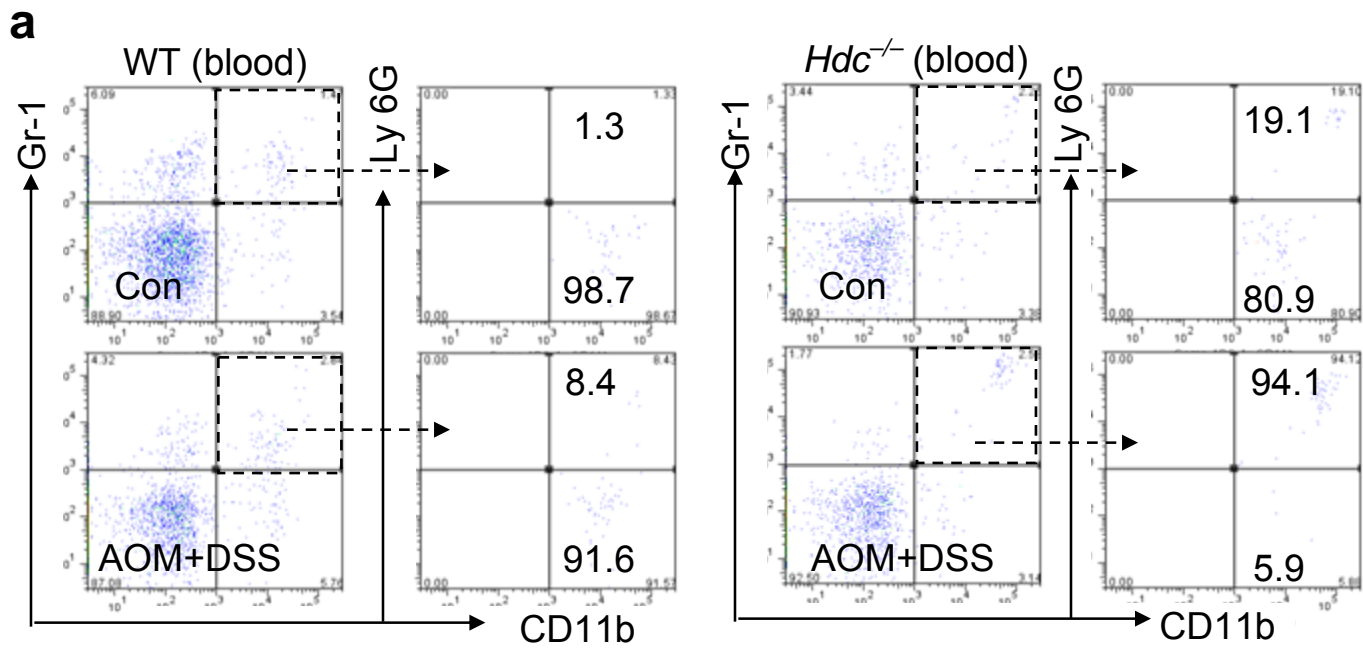
Supplementary Figure 6. *Hdc*-EGFP is predominately expressed in CD11b⁺CD49d⁻ granulocytic cells. (a–c) FACS analysis of EGFP expression in the CD11b⁺CD49d⁺ monocytic subset and CD11b⁺CD49d⁻ granulocytic subset in the peripheral blood (a), spleen (b), and bone marrow (c). The majority of *Hdc*-EGFP⁺ myeloid cells express CD11b⁺CD49d⁻ cell markers. The FACS data is representative of data from three independent experiments.



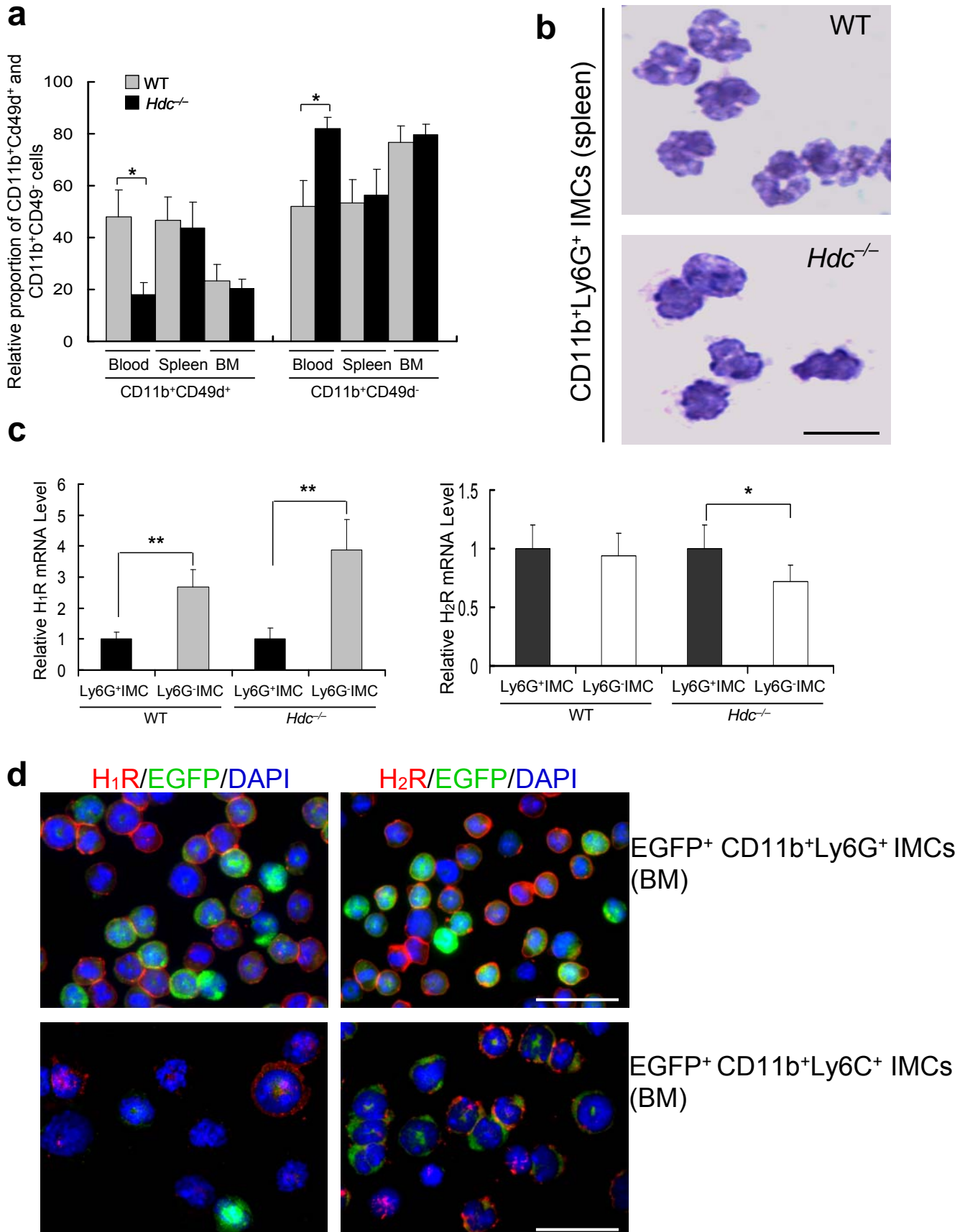
Supplementary Figure 7. *Hdc*-EGFP expression is suppressed in differentiated monocytes and macrophages. (a) Differentiation of bone marrow derived EGFP⁺ and EGFP⁻ CD11b⁺Gr-1⁺ IMCs following GM-CSF treatment as revealed by immunofluorescence and phase contrast microscopy is shown. H&E staining showed that the majority of differentiated mononuclear cells were macrophage-like (small arrowheads, top) or monocyte-like (large arrowheads, bottom). More differentiated monocyte-like or macrophage-like cells were observed in the EGFP⁻ IMCs after GM-CSF. The images are representative of data from three independent experiments. (b) Repression of *Hdc* mRNA expression with macrophage differentiation. Quantitative RT-PCR analysis confirmed the suppression of *Hdc* mRNA expression in EGFP⁺ IMCs following GM-CSF treatment (* $P < 0.01$; mean \pm s.d. from three independent experiments). (c) Schematic figure depicting the relationship of *Hdc*-EGFP⁺ cells to CD11b⁺Gr-1⁺ myeloid cells within the bone marrow.



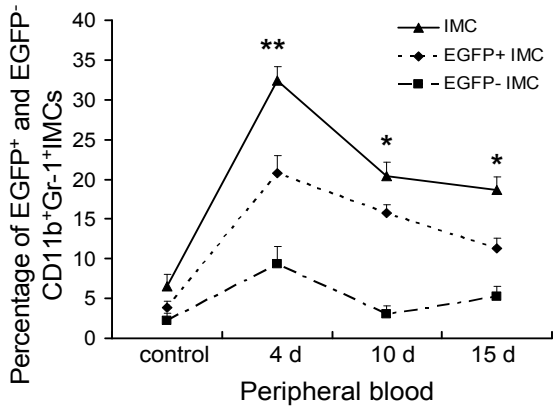
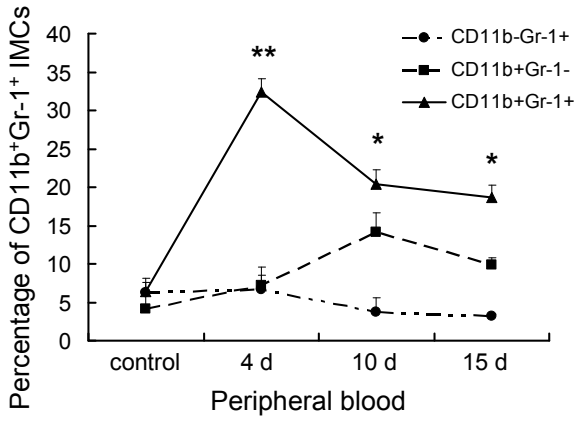
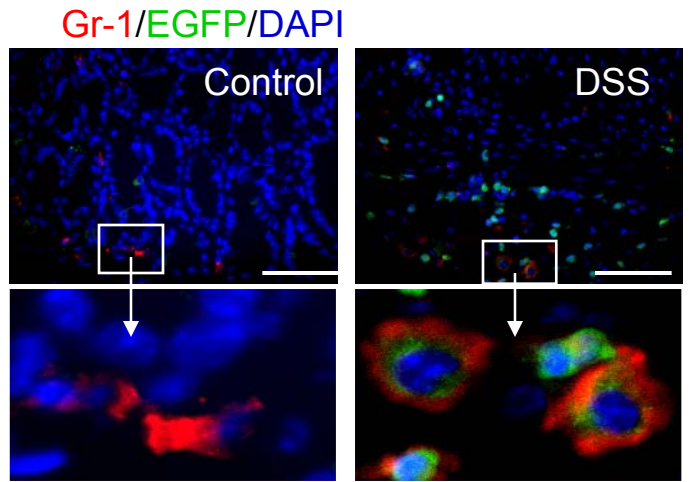
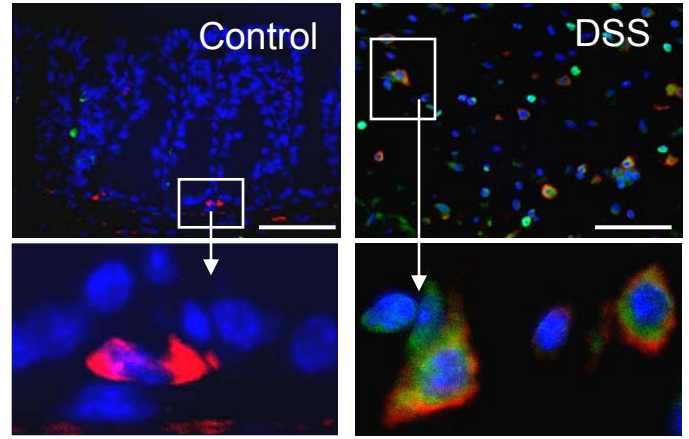
Supplementary Figure 8. Analysis of peripheral blood cells from *Hdc*^{-/-} mice by complete blood count (CBC). (a) The irreversible histamine synthesis inhibitor alpha-fluoromethylhistidine (α -FMH) (100 mg kg⁻¹, intraperitoneal injection, and daily, for 7 days) was administered to inhibit Hdc function. FACS analysis shows the expression of CD11b⁺Gr-1⁺ IMCs in the bone marrow and peripheral sites of *Hdc*-EGFP mice with temporally suppressed Hdc function (* $P < 0.05$; mean \pm s.d. $n = 5$, each group). (b–d) Quantification of leukocytes (b), red blood cells (c), and platelets (d) of WT and *Hdc*^{-/-} mice was expressed as a complete blood count (CBC) using HEMAVET 950FS (* $P < 0.05$; mean \pm s.d. $n = 5$, each group).



Supplementary Figure 9. Loss of Hdc function upregulates CD11b⁺Gr-1⁺ and CD11b⁺Ly6G⁺ IMCs and downregulates CD11b⁻Gr-1⁺ granulocytes in colon tumor-bearing *Hdc*^{-/-} mice. (a) and (b) Representative FACS data show the proportion of CD11b⁺Ly6G⁺ subset in the CD11b⁺Gr-1⁺ IMCs population in the peripheral blood (a) and spleen (b) of *Hdc*^{-/-} mice compared to wildtype mice with or without AOM + DSS-induced colon tumors. Left panel in (a) and (b) shows wildtype mice IMCs compared to *Hdc*^{-/-} IMCs in right panel. (Each group has five mice). (c) and (d) Percentage of CD11b⁺Gr-1⁻ monocytes (c) and CD11b⁻Gr-1⁺ granulocytes (d) in the peripheral blood and spleen of *Hdc*^{-/-} mice with or without AOM + DSS-induced colon tumors was measured by FACS (* *P* < 0.05; mean ± s.d. *n* = 5, each group).

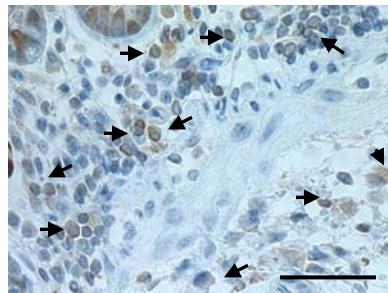
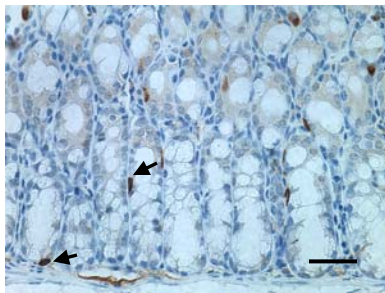


Supplementary Figure 10. Histamine regulates the differentiation of CD11b⁺Gr-1⁺ IMCs in a paracrine or autocrine manner. (a) Relative proportion of CD11b⁺CD49d⁺ monocytic and CD11b⁺CD49d⁻ granulocytic subsets in the peripheral blood, spleen, and bone marrow of *Hdc*^{-/-} mice versus wildtype mice was detected by FACS (* *P* < 0.05; mean ± s.d. *n* = 5, each group). (b) Representative haematoxylin-eosin staining of splenic CD11b⁺Ly6G⁺ granulocytes from wildtype and *Hdc*^{-/-} mice. *Hdc*^{-/-} mice showed granulocytes that were characterized by more ovoid or circular nuclei, whereas wildtype mice showed more hypersegmented nuclei (Representative figures from three independent experiments; scale bar, 20 μm). (c) Gene expression of *H₁R* and *H₂R* mRNA in CD11b⁺Gr-1⁺ IMCs. Quantitative RT-PCR analyzes of histamine receptor 1 and 2 mRNA (*H₁R* and *H₂R*) expression in the CD11b⁺Ly6G⁺ and CD11b⁺Ly6G⁻ IMCs. mRNA was analyzed from IMC subsets sorted from the bone marrow of wildtype and *Hdc*^{-/-} mice. Left panel shows *H₁R* expression while the Right panel shows *H₂R* expression (* *P* < 0.05; mean ± s.d. of three independent experiments). (d) Immunofluorescence microscopy showing expression of H₁R and H₂R in the Ly6G⁺ granulocytic subset and Ly6C⁺ monocytic subset using DAPI-stained *Hdc*-EGFP bone marrow cells. Within the EGFP-expressing myeloid population, HR expression was higher in weakly fluorescent cells than in hyperfluorescent IMCs. The images are representative of data from three independent experiments.

a**b** CD11b/EGFP/DAPI**c**

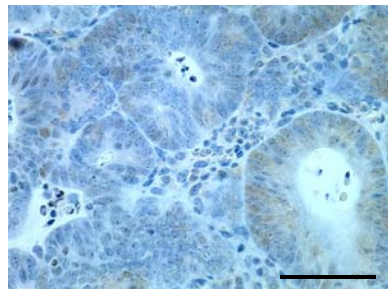
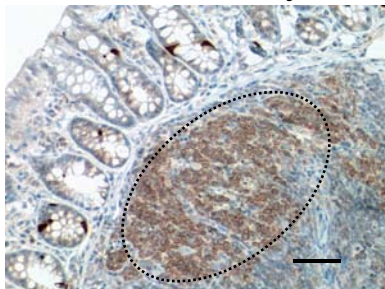
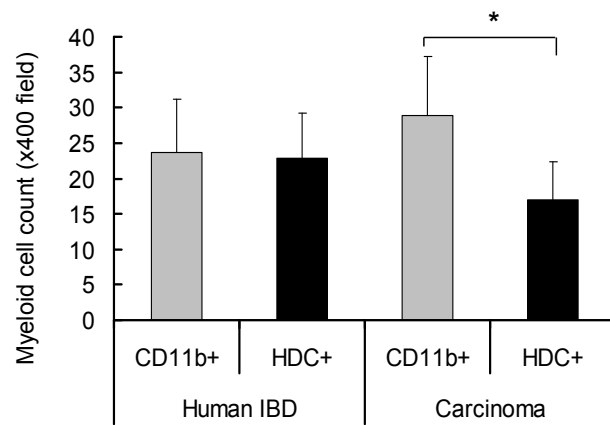
WT colon

WT distant from colon carcinoma

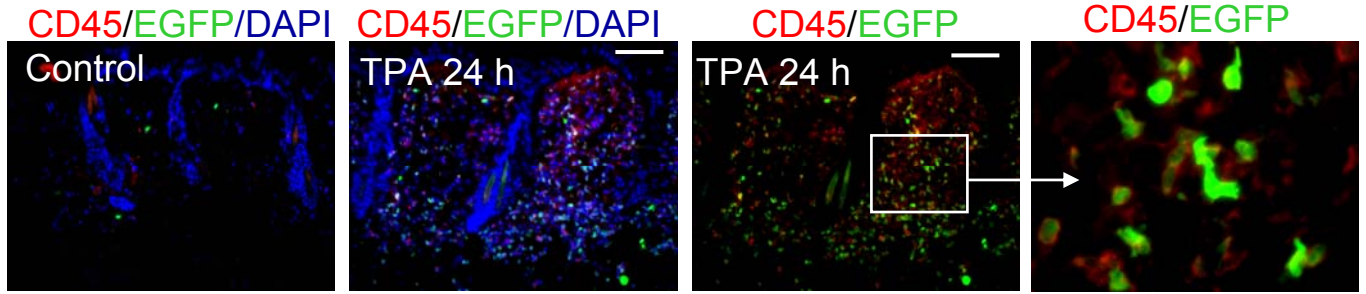
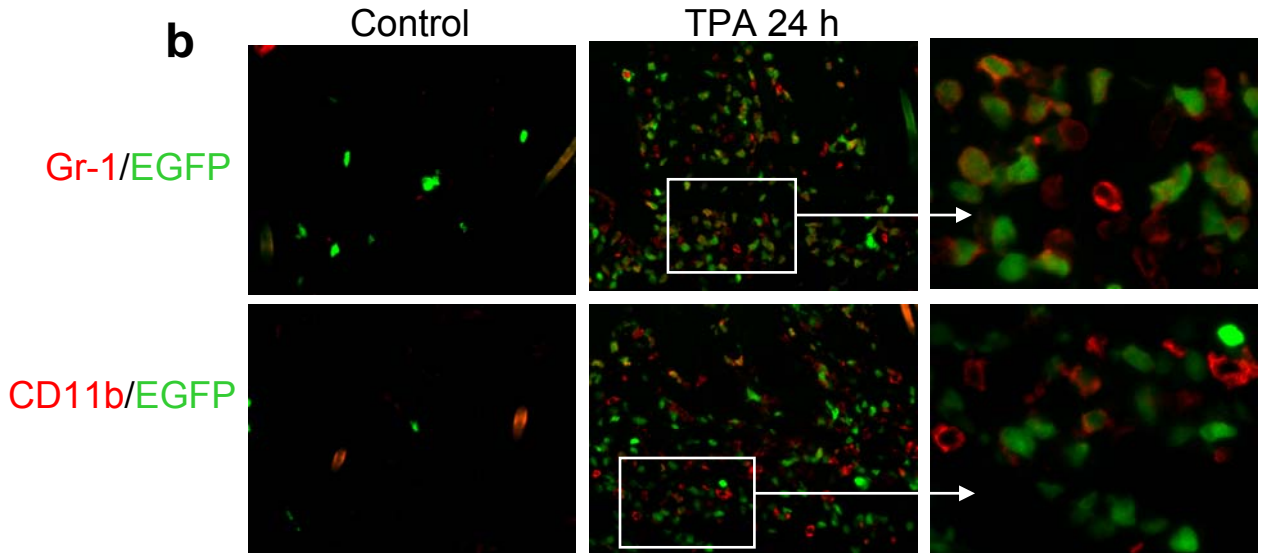
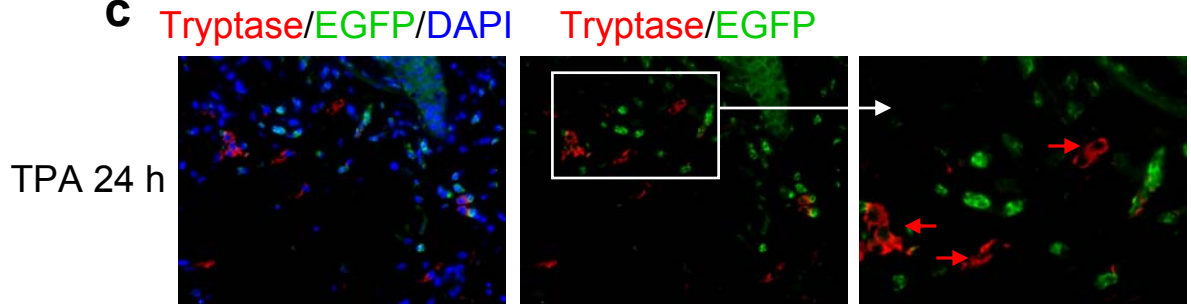
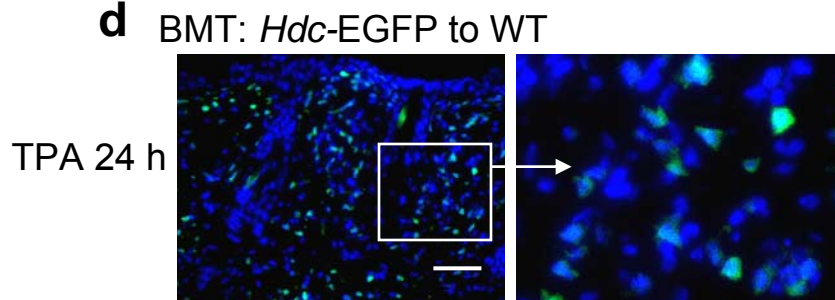


DSS 10 days

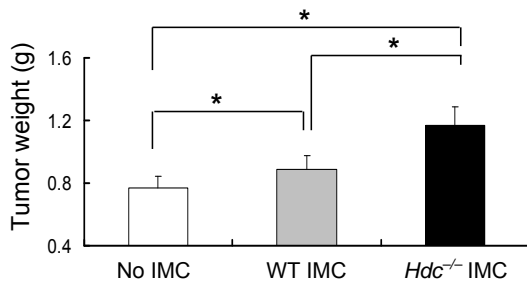
colon carcinoma

**d**

Supplementary Figure 11. EGFP-expressing CD11b⁺Gr-1⁺ IMCs are the predominant inflammatory cells in acute DSS colitis and colon tumors. (a) Effects of DSS treatment on circulating myeloid cells. FACS analysis of peripheral blood cells from *Hdc*-EGFP mice following DSS (3%) treatment. The data show significant increases in CD11b⁺Gr-1⁺ IMCs at day 4, day 10 and day 15 following DSS treatment, compared to CD11b⁺Gr-1⁻ monocytic or CD11b⁻Gr-1⁺ granulocytic myeloid cells (Top). The proportion of EGFP⁺ CD11b⁺Gr-1⁺ IMCs was markedly increased in the circulation compared to EGFP⁻ IMCs (bottom) (* $P < 0.05$; mean \pm s.d. $n = 5$, each group). (b) DSS treatment results in colonic infiltration with *Hdc*-EGFP-expressing cells. Co-localization of EGFP with CD11b (top, Texas-Red) and Gr-1 (bottom, Texas-Red)-specific antibody immuno-fluorescence of colonic tissues. (c) *Hdc*-expressing cells in the normal colon, inflamed colon, and colonic tumor of wildtype mice. Immunohistochemistry staining with *Hdc*-specific antibody revealed only a rare number of *Hdc*⁺ leukocytes in the wildtype colon (top left), compared with abundant *Hdc*⁺ inflammatory cells in acute DSS colitis (bottom left) and inflamed tissue distant from colon carcinoma (top right). Despite abundant inflammatory cells, there are markedly decreased numbers of *Hdc*⁺ leukocytes in the carcinoma (bottom right). The images are representative of data from five mice. (d) Ratio of *HDC*⁺/*CD11b*⁺ cells in human CAC compared to colitis tissue. The data represents cell counts from 15 fields from five IBD and five cancer samples (* $P < 0.05$; mean \pm s.d.).

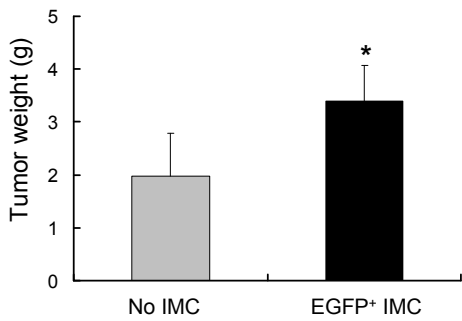
a**b****c****d**

Supplementary Figure 12. EGFP-expressing CD11b⁺Gr-1⁺ IMCs are the predominant inflammatory cells in inflamed skin induced by TPA. Immunofluorescence staining of inflamed skin of *Hdc*-EGFP mice with leukocyte markers 24 hours post TPA treatment. The figure is representative of data from analysis of five mice. **(a)** TPA treatment results in infiltration of the skin with *Hdc*-EGFP⁺ cells. Immunofluorescence shows co-localization of EGFP with the leukocyte marker CD45. More than half of the CD45⁺ cells expressed EGFP in the TPA-treated skin. **(b)** Immunofluorescence of TPA treated skin from *Hdc*-EGFP mice shows co-localization of EGFP with antibodies to CD11b and Gr-1 staining (Texas-Red). **(c)** Immunofluorescence staining shows tryptase-specific antibody positive (red) mast cells. Red arrows show cells that express tryptase alone. **(d)** Immunofluorescence images of DAPI stained skin from a bone marrow transplanted mouse 24 hours post TPA showing that a large number of infiltrating EGFP⁺ inflammatory cells are bone marrow derived (Donor: *Hdc*-EGFP mice; recipient: wildtype B6 mice).

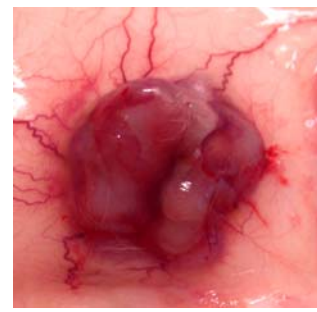
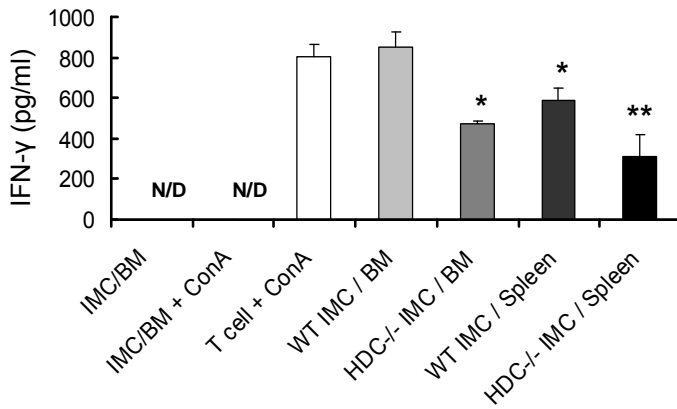
aImplanted CD11b⁺Gr-1⁺ IMCs

No IMC

WT IMC

Hdc^{-/-} IMC**b**

Control: no IMC

EGFP⁺
CD11b⁺Gr-1⁺ IMC**c**

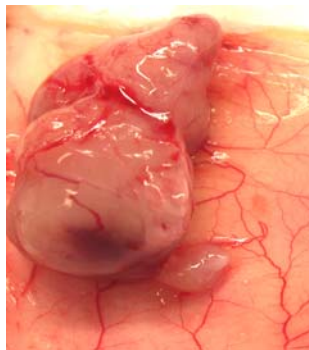
Supplementary Figure 13. CD11b⁺Gr-1⁺ and CD11b⁺Ly6G⁺ IMCs from bone marrow of *Hdc*^{-/-} mice accelerate tumor growth. (a) Colon cancer cell CT26 co-implanted with CD11b⁺Gr-1⁺ IMCs isolated from the bone marrow of wildtype and *Hdc*^{-/-} mice in NOD-SCID mice and tumor weight measures. On the right, representative images are shown from each group ($n = 6$, * $P < 0.05$ compared to control). (b) Similar to (a), *Hdc*-EGFP-expressing CD11b⁺Gr-1⁺ IMCs isolated from the bone marrow of *Hdc*-EGFP mice and co-implanted with CT26 cells in NOD-SCID mice. On the right, a representative image shows a large number of new blood vessels were observed in EGFP⁺ IMCs co-implanted tumors ($n = 6$, * $P < 0.05$ compared to control group). Representative pictures are shown for each group. (c) Measurement of IFN- γ in the supernatant of CD4⁺ T cells co-cultured with CD11b⁺Gr-1⁺ IMCs by ELISA. CD11b⁺Gr-1⁺ IMCs were sorted from the bone marrow of colon tumor-bearing wildtype and *Hdc*^{-/-} mice. CD4⁺ T cells were sorted from the spleen of wildtype mice. IMCs (0.25 million per well) and T cells (0.25 million per well) were co-cultured in the anti-CD3e precoated 24-well plate with Concanavalin A culture medium (5 $\mu\text{g ml}^{-1}$) for 72 hours and supernatant harvested for ELISA measurement (* $P < 0.05$, ** $P < 0.01$ compared to T cell control group).



Control:
No CD11b⁺Ly6G⁺ IMCs



WT:
CD11b⁺Ly6G⁺ IMCs



Hdc^{-/-}:
CD11b⁺Ly6G⁺ IMCs

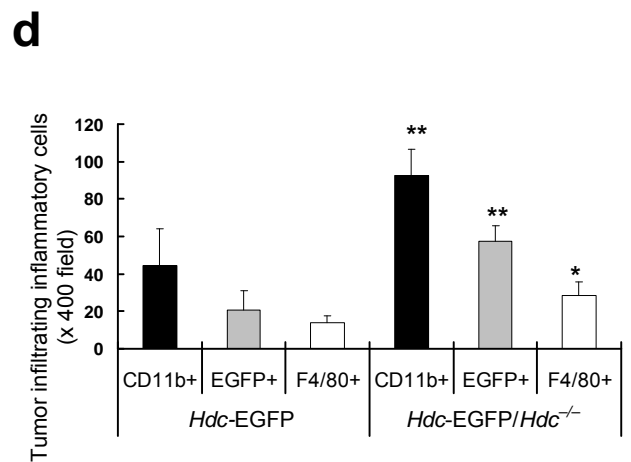
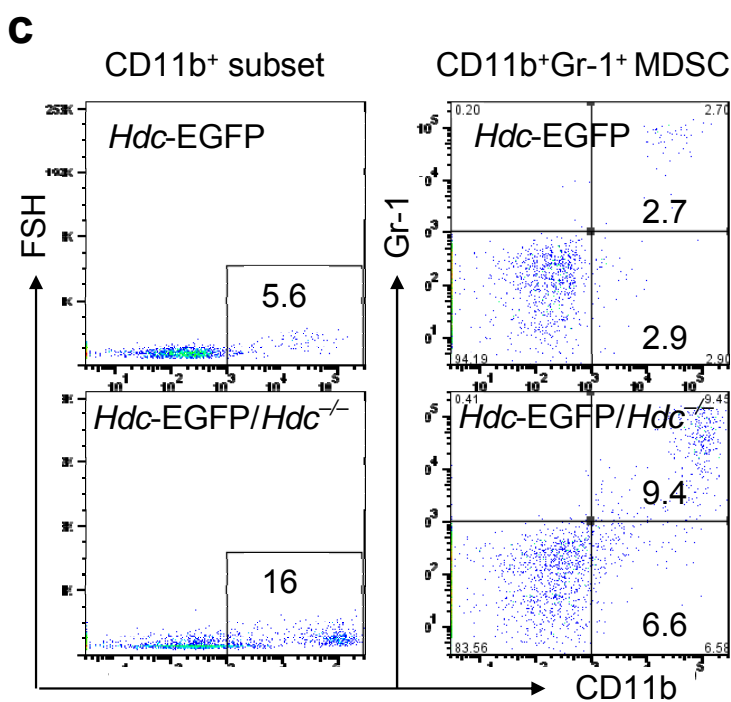
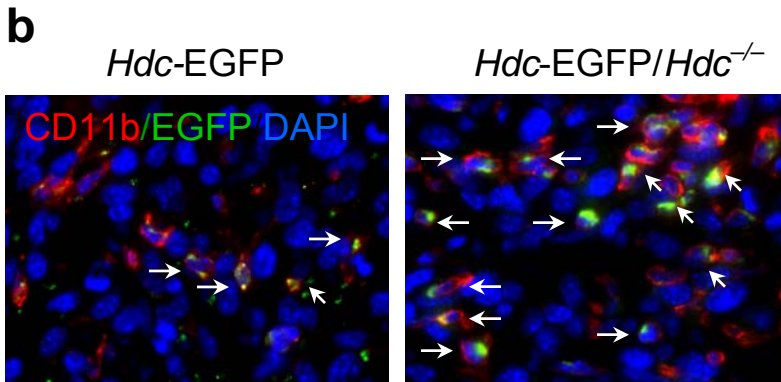
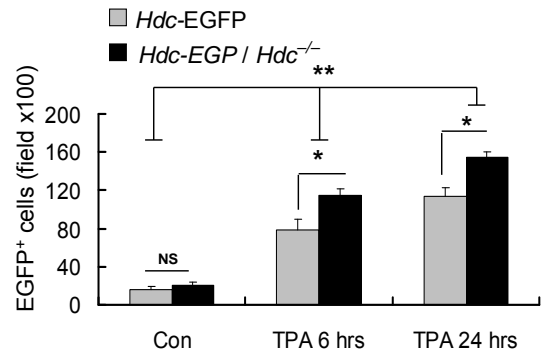
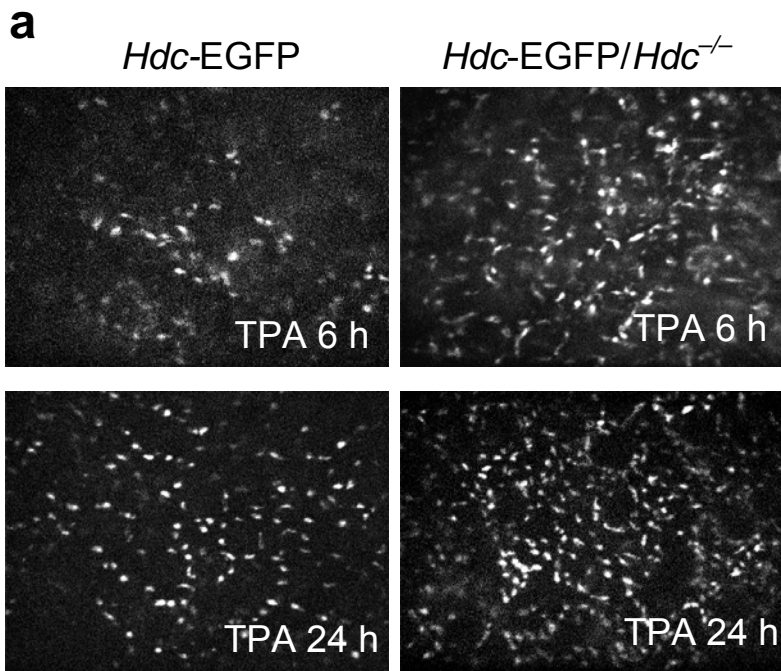


Hdc^{-/-}: IMCs
plus histamine

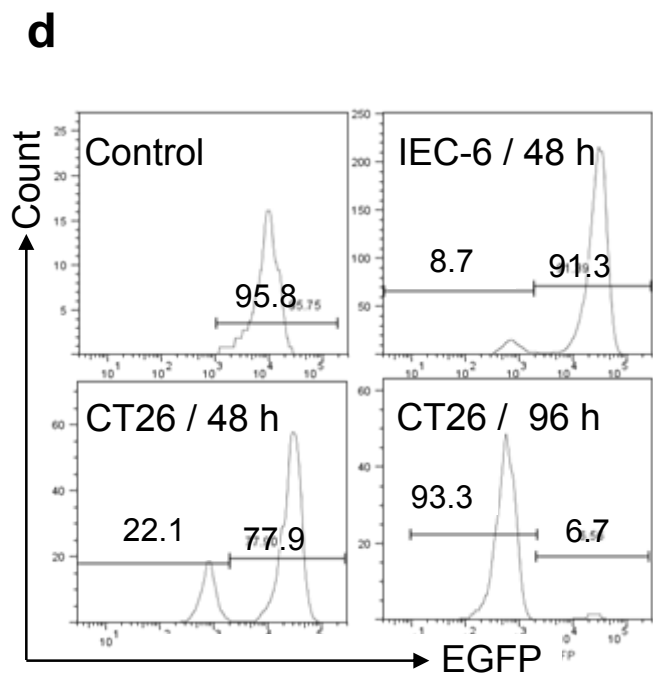
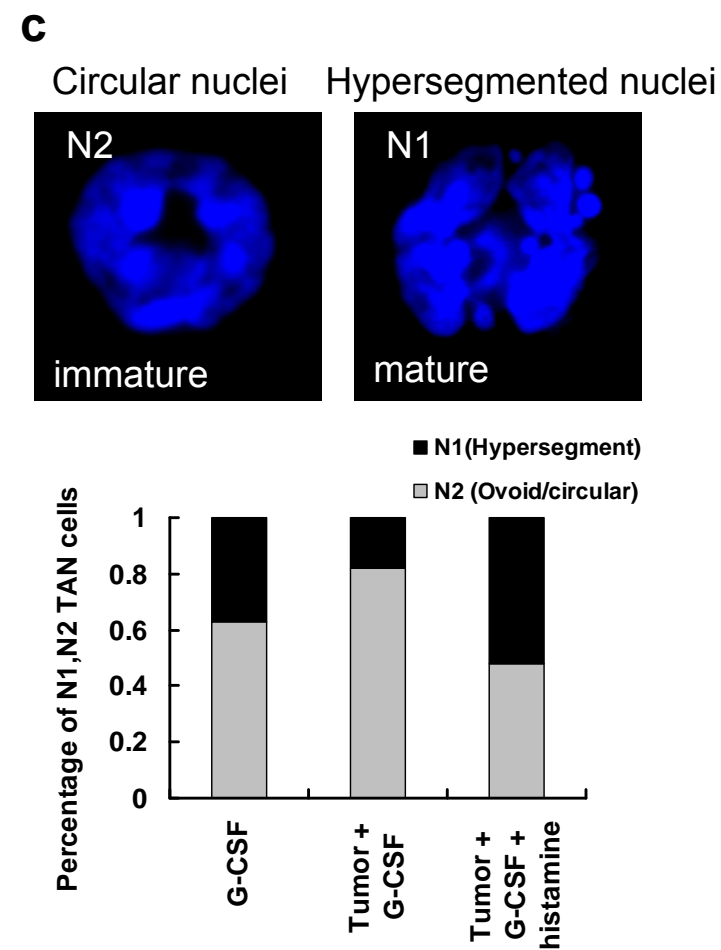
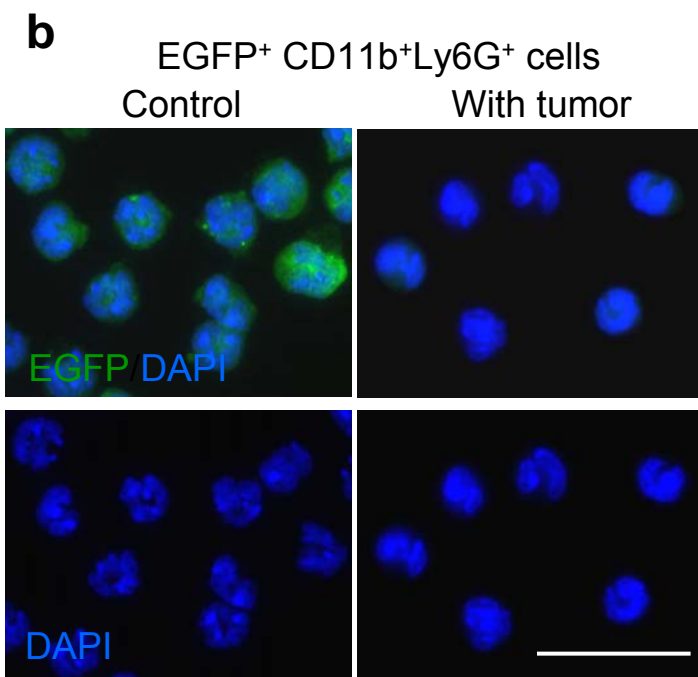
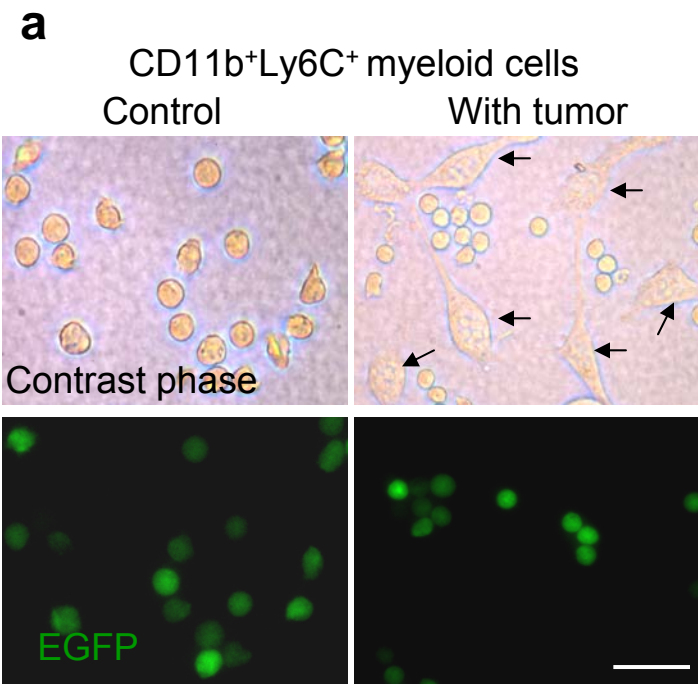


IL-6^{-/-}:
CD11b⁺Ly6G⁺ IMCs

Supplementary Figure 14. CD11b⁺Ly6G⁺ IMCs from the bone marrow of *Hdc*^{-/-} mice promote angiogenesis and tumor growth. Representative images of CT26 xenograft tumors co-implanted with different sources of CD11b⁺Ly6G⁺ IMCs. The pictures show the tumor size and number of vessel branch points of xenograft tumors. The xenograft tumors include control (No IMCs), IMCs (WT), IMCs (*Hdc*^{-/-}), IMCs (*Hdc*^{-/-}) plus histamine, and IMCs (*IL-6*^{-/-}) groups. (Representative pictures are shown from total seven tumors of each group).

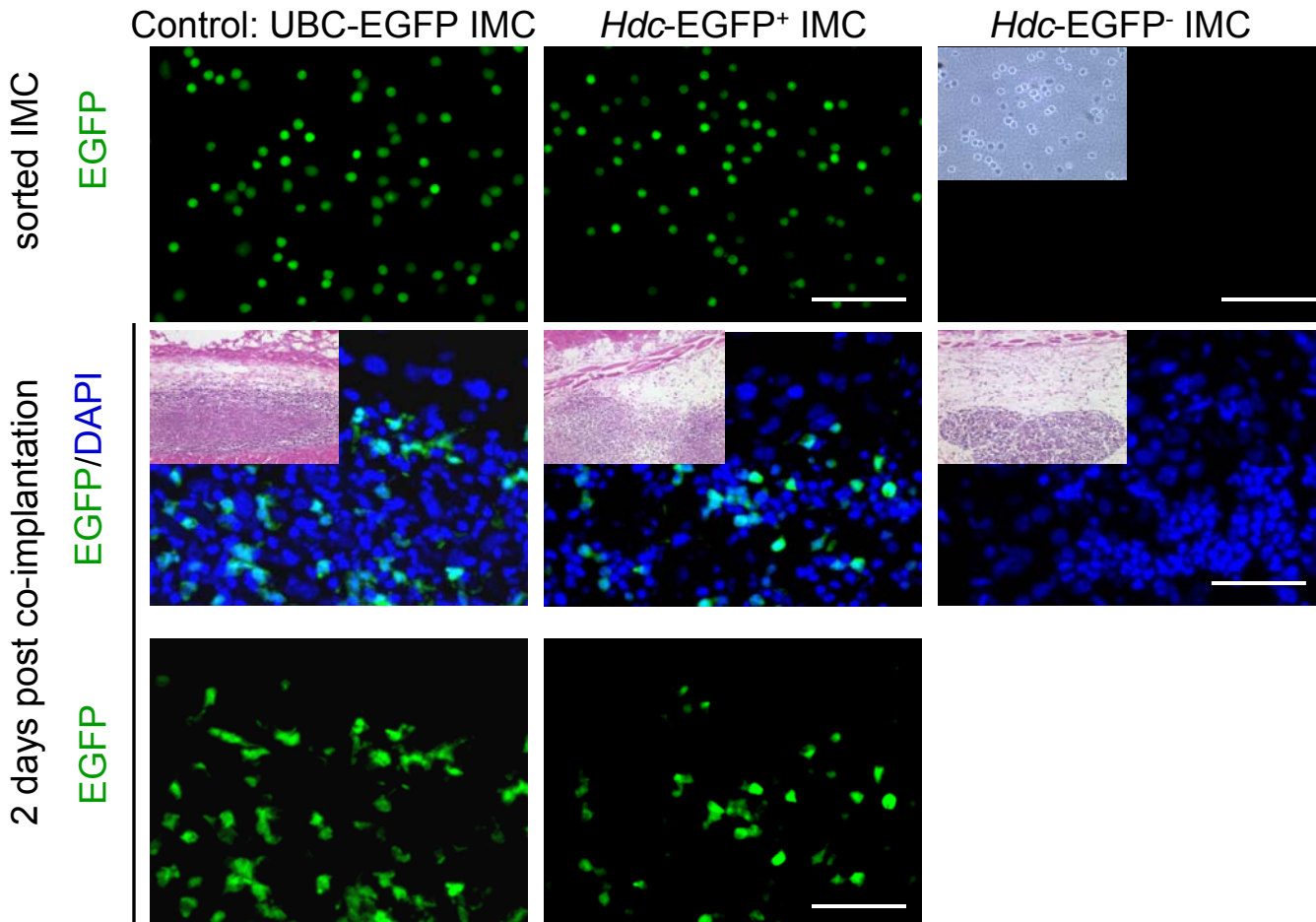


Supplementary Figure 15. *Hdc*-EGFP-expressing cells are rapidly recruited by carcinogens and histamine deficiency promotes EGFP-expressing CD11b⁺Ly6G⁺ IMC migration. (a) Representative images for the real-time intravital microscopy of *Hdc*-EGFP⁺ cells in the skin. On the right, EGFP⁺ inflammatory cells were quantified (five images per mouse) in the ears of *Hdc*-EGFP and *Hdc*-EGFP/*Hdc*^{-/-} mice (C57BL/6 and Balb/C mixed background) at 6 h and 24 h following TPA treatment. (Data are representative of three independent experiments). (b) and (c) Effect of histamine-deficiency on the mobility of EGFP-expressing CD11b⁺Ly6G⁺ IMCs. Colon cancer CT26 cells (1 X 10⁶ cells) were subcutaneously injected in the dorsum skin of NOD-SCID mice (*n* = 4) and xenograft tumors (0.7 cm X 0.7 cm) could be observed 10 days later. EGFP-expressing CD11b⁺Gr-1⁺ IMCs were sorted from the bone marrow of wildtype and *Hdc*^{-/-} background mice and the same number of EGFP⁺ cells (2.5 X 10⁶ cells) were administrated by tail intravenous injection. The xenograft tumors were collected for analysis 24 h later. Immuno-costaining with GFP and CD11b-specific antibodies confirmed increased EGFP⁺CD11b⁺ myeloid cells in *Hdc*^{-/-} mice (b). FACS data shows an approximately 3-fold increase in CD11b⁺ myeloid cells and CD11b⁺Gr-1⁺ IMCs in the *Hdc*^{-/-} xenograft tumors (c). (d) Inflammatory cells in the xenograft tumors. CD11b⁺ inflammatory cells, EGFP⁺ IMCs, and F4/80⁺ macrophages were counted in the xenograft tumors. (5–7 fields of each tumor; a total of four tumors from WT and *Hdc*^{-/-} group were counted. * *P* < 0.05, ** *P* < 0.01 compared to WT group).



Supplementary Figure 16. Co-culture with tumor cells downregulates *Hdc*-EGFP expression in immature myeloid cells. (a) Co-culture of EGFP-expressing CD11b⁺Ly6C⁺ monocytic IMCs with CT26 cells. Left shows control, right exhibits loss of *Hdc*-EGFP fluorescence in these monocyte-like cells following 48 h culture. (Arrows indicated cells in the top right). (b) Co-culture of EGFP-expressing CD11b⁺Ly6G⁺ granulocytic IMCs with CT26 cells. Left shows control, EGFP expression in EGFP-expressing CD11b⁺Ly6G⁺ IMCs was detected with DAPI stained (top right). Nuclear morphology was examined by DAPI staining (bottom right). The images shown are representative of data from three independent experiments. (c) Exogenous histamine promotes differentiation and maturation of CD11b⁺Ly6G⁺ TANs. The top pictures show nuclear morphology of CD11b⁺Ly6G⁺ IMCs in different stages with DAPI fluorescence staining: immature (ovoid or circular nucleus, N2 type) and mature (hypersegmented nucleus, N1 type). The bottom graph shows differentiation and maturation of bone marrow derived EGFP-expressing CD11b⁺Ly6G⁺ IMCs with G-CSF, G-CSF + CT26 tumor cells, and G-CSF + CT26 tumor cells + histamine 48 h respectively. Cells were collected and fixed with 2% PFA solution 2 h and stained with DAPI. The numbers of immature cells with ovoid or circular nuclei and mature cells with hypersegmented nuclei were counted by immunofluorescence microscopy (high magnification, x 900) (The average value was calculated from at least twelve pictures of three independent experiments). (d) FACS analysis for EGFP expression in the bone marrow-derived EGFP-expressing CD11b⁺Ly6G⁺ IMCs co-cultured with the cancer cell line CT26 at 48 h and 96 h. CD11b⁺Ly6G⁺ IMCs co-cultured with the rat intestinal epithelial cells IEC-6 or no IMCs (as controls). The figures shown representative of data from three independent experiments.

Implanted CD11b⁺Gr-1⁺ IMCs sorted from
BM of UBC-EGFP or *Hdc*-EGFP mice



Supplementary Figure 17. Tracking *Hdc*-EGFP-expressing CD11b⁺Gr-1⁺ IMCs in xenograft tumors. *In vivo* tracking of *Hdc*-EGFP expression in EGFP⁺ and EGFP⁻ CD11b⁺Gr-1⁺ IMC subsets. UBC-EGFP⁺ CD11b⁺Gr-1⁺ IMCs were used to track exogenous IMCs as co-implanted controls (in the left). Right shows EGFP⁻ IMCs. TOP: The images show IMCs sorted from the bone marrow of UBC-EGFP (a) and *Hdc*-EGFP⁺ IMCs (b) and *Hdc*-EGFP⁻ IMCs from *Hdc*-EGFP mice. Middle and bottom: Representative images show EGFP expression with DAPI stained xenograft tumors two days post implantation. (1.0×10^6 EGFP⁺ IMCs and 2.0×10^6 CT26 cells were co-implanted in the bank of NOD-SCID mice). Inset shows H&E staining of tumor sections. The images are representative of data from three mice.